

Introduction

Atmospheric turbulence causes refractivity fluctuations that might be observed e.g. in post-fit residuals of carrier phase observations or in estimated zenith tropospheric signal delays (ZTD). Since undifferenced carrier phase observations contain superpositions of several effects (such as residual receiver and satellite clock variations, receiver noise, multipath, and turbulence effects) the separation of these effects is a challenging task. In this study, we show results from Precise Point Positioning (PPP) analyses using different GPS-receivers both with and without ultra-stable frequency standards. For ultra-stable frequency standards enhanced clock modelling approaches can be applied (Weinbach et al., 2011) that improve the separability of receiver clock parameters and tropospheric delays. For two exemplary IGS stations we demonstrate the effect of clock modelling on the stochastic properties of tropospheric zenith delays and carrier phase residuals in terms of their structure functions and power spectra.

Characterisation of high-frequency carrier phase and ZTD fluctuations

A common method to characterise fluctuations of both phase observations Φ and tropospheric delay estimates T is the temporal structure function (as a function of time lag τ):

$$D_x(\tau) = \langle [x(t + \tau) - x(t)]^2 \rangle$$

Double-logarithmic plots of structure functions typically show straight line segments that reveal the noise type of the corresponding stochastic process. Turbulence theory predicts a power-law behaviour with exponents (i.e., straight line slopes) ranging from 5/3 for small separations τ and finally reaching 0 for large τ (Wheelon, 2001).

Precise Point Positioning (PPP) analyses

As an example, 5 s data of two IGS stations (AMC2 with H-maser and ARTU with an internal quartz oscillator) with the same receiver types (Ashtech Z-XII3(T)) but different frequency standards has been analysed by a Kalman filter PPP-approach. For the analyses, data from day 2011/01/04 has been used with an elevation cut-off angle of 5 degrees, using precise orbit and 5 s satellite clock products from CODE, and elevation dependent weighting. The ZTD process noise is set to an average literature value of $5 \text{ mm}/\sqrt{h}$. Clock modelling is performed by using clock system noise derived from Allan variance parameters (van Dierendonck et al., 1984). Further PPP results can be found in Vennebusch et al., 2011.

Example: H-maser frequency standard (AMC2)

Figure 1 shows the receiver clock offsets of AMC2 both with and without clock modelling as well as its impact on ZTD structure functions and ZTD power spectra. The smooth clock offset time series obtained by clock modelling (red line) may be considered as closer to the 'true' clock behaviour while the other time series (black line) contains contributions from effects such as multipath, observation noise, and possibly high-frequency ZTD variations. With clock modelling these high-frequency effects are transferred into the ZTD time series. This is especially obvious from the different power spectra.

The carrier phase residuals with and without clock modelling show only small differences that can most clearly be seen in the structure functions values for small time lags. In the original time series these effects are masked by dominating systematic errors such as multipath.

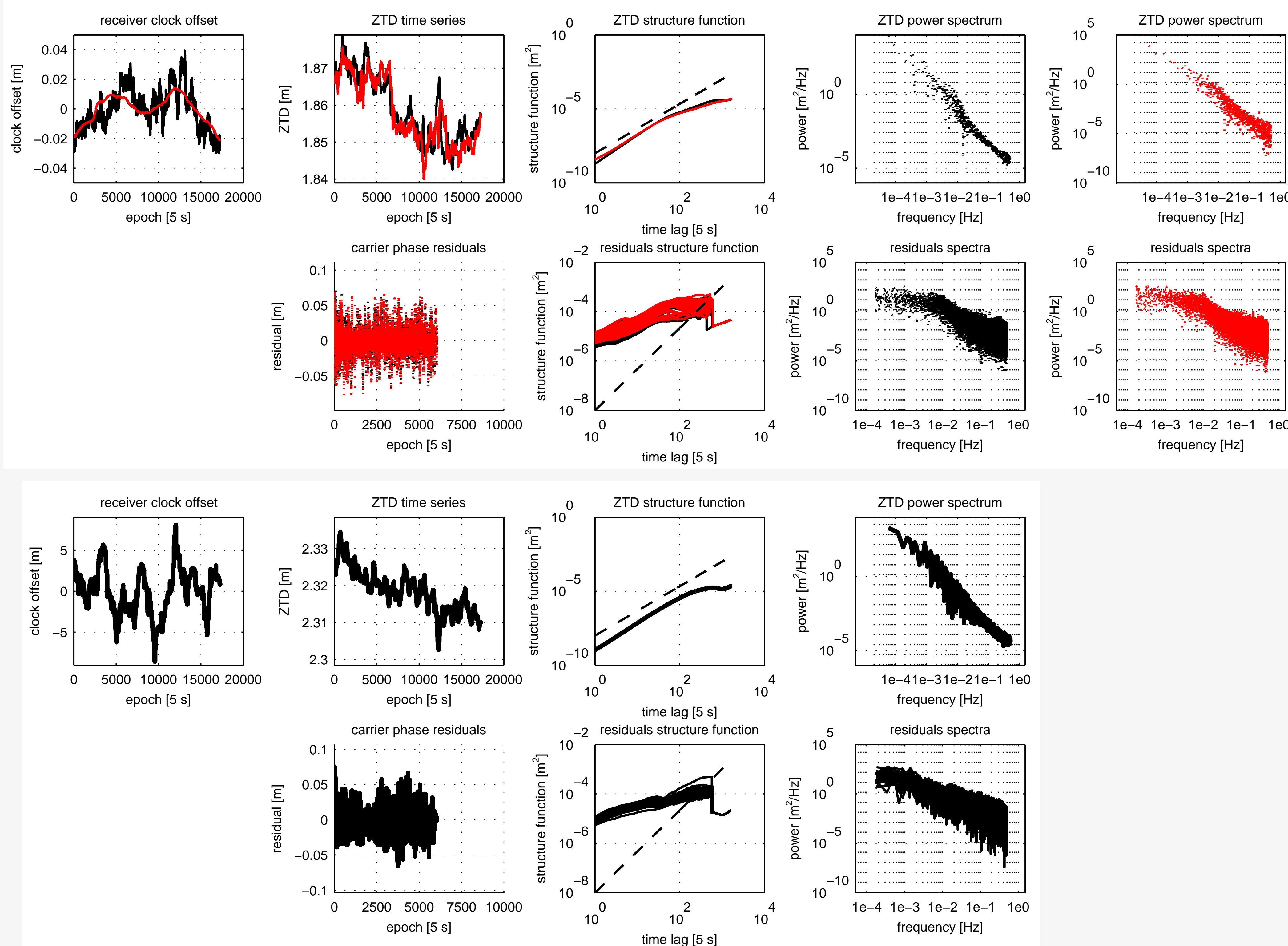


Fig. 1: PPP results for IGS station AMC2. The black lines show the respective results obtained without clock modelling, while the red lines demonstrate the effect of enhanced clock modelling. The dashed lines in the structure function plots demonstrate a reference 5/3-power law behaviour.

Fig. 2: PPP results for IGS station ARTU. Only results without clock modelling are shown. The dashed lines in the structure function plots demonstrate a reference 5/3-power law behaviour.

Example: Quartz oscillator (ARTU)

For station ARTU, clock modelling is not appropriate since the internal quartz frequency standard can not be modelled as a stable clock. Thus, figure 2 shows the clock offset basically estimated epoch-by-epoch and with the typical large variations of an ordinary quartz oscillator steered to GPS time. Figure 2 also shows tropospheric delays, their structure function and power spectrum. Compared to the results from AMC2, only small differences can be seen. Again, the ZTD structure function shows a 5/3-power law behaviour and the residuals are a bit more noisy as shown by the slightly larger structure function values for small time separations.

Conclusions

- Using ultra-stable frequency standards together with improved clock modelling leads to more realistic filter modelling and improves separability of error effects,
- Clock modelling has no significant impact on the 5/3 power-law behaviour of ZTD,
- A 5/3 power-law behaviour as predicted by turbulence theory can be observed in ZTD structure function,
- Detection of atmospheric turbulence in carrier phase residuals requires further investigations of the remaining unmodelled effects such as multipath.

References

- van Dierendonck AJ, McGraw JB, Brown RG: Relationship between Allan variances and Kalman filter parameters, Proc. 16th PTTI Applications and Planning Meeting, NASA, Nov. 27-29, 1984.
- Vennebusch M, Schön S, Weinbach U: Temporal and spatial stochastic behaviour of high-frequency slant tropospheric delays from simulations and real GPS data, Advances in Space Research, Vol. 47 (10): 1681-1690, Elsevier, 2011.
- Weinbach U, Schön S: GNSS receiver clock modeling when using high-precision oscillators and its impact on PPP, Advances in Space Research, Vol. 47 (2): 229-238, Elsevier, 2011.
- Wheelon AD: Electromagnetic scintillation-I. Geometrical optics, Cambridge University Press, Cambridge, 2001.

Acknowledgments

The authors thank the German Research Foundation (DFG) for its financial support (SCHO 1314/1-1).